Accepted by ApJ Letters on February 14, 2011
Preprint typeset using LaTeX style emulateapj v. 11/10/09

arXiv:1007.0661v2 [astro-ph.CO] 14 Mar 2011

PROGENITOR DIAGNOSTICS FOR STRIPPED CORE-COLLAPSE SUPERNOVAE: MEASURED METALLICITIES AT EXPLOSION SITES

M. Modjaz[1,2], L. Kewley[3], J. S. Bloom[1,4], A. V. Filippenko[1], D. Perley[1], and J. M. Silverman[1,5]

Accepted by ApJ Letters on February 14, 2011

ABSTRACT

Metallicity is expected to influence not only the lives of massive stars but also the outcome of their deaths as supernovae (SNe) and gamma-ray bursts (GRBs). However, there are surprisingly few direct measurements of the local metallicities of different flavors of core-collapse SNe. Here we present the largest existing set of host-galaxy spectra with H II region emission lines at the sites of 35 stripped-envelope core-collapse SNe. We derive local oxygen abundances in a robust manner in order to constrain the SN Ib/c progenitor population. We obtain spectra at the SN sites, include SNe from targeted and untargeted surveys, and perform the abundance determinations using three different oxygen-abundance calibrations. The sites of SNe Ic (the demise of the most heavily stripped stars, having lost both H and He layers) are systematically more metal rich than those of SNe Ib (arising from stars that retained their He layer) in all calibrations. A Kolmogorov-Smirnov test yields the very low probability of 1% that SN Ib and SN Ic environment abundances, which are different on average by $\sim$0.2 dex (in the Pettini & Pagel scale), are drawn from the same parent population. Broad-lined SNe Ic (without GRBs) occur at metallicities between those of SNe Ib and SNe Ic. Lastly, we find that the host-galaxy central oxygen abundance is not a good indicator of the local SN metallicity; hence, large-scale SN surveys need to obtain local abundance measurements in order to quantify the impact of metallicity on stellar death.

Subject headings: galaxies: abundances— supernovae: general

1. INTRODUCTION

Understanding the progenitors of the most energetic cosmic explosions, particularly gamma-ray bursts (GRBs) and supernovae (SNe), is a grand pursuit. Known already from their spectra is that stripped-envelope core-collapse SNe (CCSNe; "stripped SNe" hereafter) have progressively (from Types IIb to Ib to Ic) larger amounts of their outer hydrogen and helium envelopes removed prior to explosion (e.g., Clocchiatti et al. 1996; Filippenko 1997). However, the dominant mechanism of stripping is not well known, nor are basic quantities such as the mass and metallicity of their stellar progenitors. The exciting connection between long-duration GRBs and broad-lined SNe Ic (SNe Ic-bl) and the existence of SNe Ic-bl without observed GRBs (see Woosley & Bloom 2006 for a review) raises the question of what distinguishes a GRB progenitor from that of an ordinary SN Ic-bl without a GRB. Clear knowledge of the stellar progenitors of various explosions is essential for understanding the endpoints of stars over a broad mass range and for mapping the chemical enrichment history of the universe (Nomoto et al. 2006).

Two progenitor channels have been proposed for stripped SNe: either single massive Wolf-Rayet (WR) stars with main-sequence (MS) masses of $\gtrsim 30$ M$_\odot$ that have experienced mass loss during the MS and WR stages (e.g., Filippenko & Sargent 1985; Woosley et al. 1993), or binaries from lower-mass He stars that have been stripped of their outer envelopes through interaction (Podsiadlowski et al. 2004, and references therein), or a combination of both. Attempts to directly identify SN Ib/c progenitors in pre-explosion images have not yet been successful (e.g., Gal-Yam et al. 2005; Maund et al. 2005; Smartt 2009).

A more indirect but very powerful approach is to study the environments of a large sample of CCSNe in order to discern systematic trends that characterize their stellar populations. SNe Ic tend to be found in the brightest regions of their host galaxies (Kelly et al. 2008) and are more closely associated with H II regions than SNe II (Anderson & James 2008, and references therein). SNe Ib also tend to be found in bright regions of their respective hosts, less closely coupled than SNe Ic but more so than SNe II. This evidence suggests the progenitors of SNe Ib/c may thus be more massive than those of SNe II, which are $\sim$ 8–16 M$_\odot$ (see Smartt 2009 for a review). Other studies attempt to measure the metallicity by using the SN host-galaxy luminosity as a proxy (Prantzos & Boissier 2003; Arcavi et al. 2010), or by using the metallicity of the galaxy center measured from Sloan Digital Sky Survey (SDSS) spectra (Prieto et al. 2008) to extrapolate to that at the SN position (Boissier & Prantzos 2009).

Those prior metallicity studies do not directly probe the local environment of each SN (which is different from the galaxy center due to metallicity gradients), nor do they differentiate between the different SN subtypes. Here we present a statistically significant sample of stripped SNe (SNe IIb and Ib, SNe Ic, and SNe Ic-bl) with robust, uniform, and direct determinations of their

---

[1] Department of Astronomy, University of California, Berkeley, CA 94720-3411; Miller Fellow.
[2] Columbia Astrophysics Lab, Columbia University, NYC, NY 10024; Hubble Postdoctoral Fellow.
[3] University of Hawaii, 2680 Woodlawn Drive, Honolulu, HI 96822.
[4] Sloan Research Fellow.
[5] Marc J. Staley Fellow.

local metallicity in order to quantify the impact of metallicity on massive stellar deaths, building on our previous work (Modjaz et al. 2008). We note that in the final stages of this research, Anderson et al. (2010) reported on a similar topic; we briefly note the differences in the sample and results below.

2. THE SUPERNOVA SAMPLE AND ASSOCIATED HOST GALAXIES

In Table 1, we present the SN sample for which we measured local metallicities. It consists of 35 low-redshift ($z < 0.18$) stripped SNe, selected from the International Astronomical Union Circulars (IAUCs)[6] according to the following criteria: (1) well-determined SN subtype, (2) discovered in targeted and untargeted surveys, and (3) H II region emission at the position of the SN (within our slit width of $1''$, see § 3), as seen in our spectra, with which to directly determine the metallicity at the SN site. We discuss the potential impact of our selection effects in § 5.1. While our sample is heterogeneous and not complete, we have good reasons to believe that it gives a fair representation of the kinds of environments that give rise to observed stripped CCSNe. Besides having SNe from traditional searches (e.g., the Lick Observatory SN Search; Filippenko et al. 2001) that target luminous galaxies, we include SNe from untargeted surveys (e.g., SDSS, Nearby SN Factory; see Modjaz et al. 2008 for more detailed discussion) in order to mitigate any potential metallicity bias: since SN host galaxies in targeted searches are preferentially more luminous, they are usually also more metal rich (Tremonti et al. 2004).

Furthermore, we include host-galaxy spectra of the broad-lined SNe Ic without observed GRBs presented by Modjaz et al. (2008), which were reduced and analyzed in the same fashion as the data presented here. For completeness, we also include metallicity measurements of all spectroscopically confirmed GRB-SNe (Modjaz et al. 2008, and references therein; Christensen et al. 2008; Chornock et al. 2010; Starling et al. 2010).

The total sample of SNe Ib, Ic, and Ic-bl whose local metallicities we are analyzing here amounts to 47 SNe (without observed GRBs).

3. OPTICAL SPECTROSCOPIC OBSERVATIONS

Optical long-slit ($1''$ wide) spectra of the locations of faded SNe were obtained with the 10-m Keck I telescope using the Low Resolution Imaging Spectrometer (LRIS; Oke et al. 1995) plus atmospheric dispersion corrector (ADC) on a number of nights 2007–2010. We generally employed a combination of the 300/5000 grism on the blue-side CCD and the 400/8500 grating on the red-side CCD Here we also include our Keck LRIS/ADC observations of stripped CCSNe in those cases where superimposed H II region emission lines were visible in the SN spectra (e.g., Modjaz et al. 2009; Silverman et al. 2009).

All optical spectra were reduced and calibrated with standard techniques in IRAF and our own IDL routines for flux calibration (Matheson et al. 2008). For cases where the SN was still present, we eliminated the SN contribution following the successful method of Modjaz et al. (2008). After correcting all spectra for their recession velocities we measured optical emission-line fluxes by fitting Gaussians to the individual lines via the *splot* routine in IRAF. For the derivation of the statistical errors, which typically amount to 5–10% of the emission-line fluxes, we follow Pérez-Montero & Díaz (2003) and, in part, Rupke et al. (2010).

4. METALLICITY MEASUREMENTS

The nebular oxygen abundance is the canonical choice of metallicity indicator for studies of the interstellar medium (ISM), since oxygen is the most abundant metal, only weakly depleted, and exhibits very strong nebular emission lines in the optical wavelength range (e.g., Tremonti et al. 2004). Using our measured line fluxes of [O II], [O III], [N II], Hα, and Hβ, we correct for reddening via the Balmer decrement and the standard Galactic reddening law with $R_V = 3.1$ (Cardelli et al. 1989), and compute the gas-phase oxygen abundance via strong-line diagnostics.

We employ three independent and well-known calibrations: (1) the iterative method of Kewley & Dopita (2002), as updated by Kewley & Ellison (2008) (henceforth KD02-comb); (2) the calibration by McGaugh (1991) (henceforth M91); and (3) the diagnostic of Pettini & Pagel (2004) (both PP04-O3N2 and N2), which is close to the direct electron temperature (T_e) scale. Moreover, we compute the uncertainties in the measured metallicities by explicitly including the statistical uncertainties of the line-flux measurements and those in the derived SN host-galaxy reddening, and propagate them into the metallicity determination. Since the PPO4-O3N2 scale utilizes ratios of lines that are very close in wavelength, the effects of uncertain reddening and scaling between the blue and red LRIS CCDs have negligible impact on the abundance measurements (something we tested). The independently published metallicities of SNe 2006jc (Pastorello et al. 2007), 2007uy, and 2008D (Thöne et al. 2009) agree with our values within the uncertainties.

5. RESULTS

Figure 1 shows the cumulative distributions of local metallicities in each of the three scales for different types of stripped CCSNe: the ordinate indicates the fraction of the SN population with metallicities less than the abscissa value. The SN subtypes shown are SNe Ib (including SNe IIb), Ic, and Ic-bl (without observed GRBs), and their respective numbers for which the requisite emission lines for that diagnostic were available are given in the legend. Furthermore, we show confidence bands around each cumulative trend, which we computed via bootstrap with 10,000 realizations based on our metallicity measurements and their associated uncertainties. The metallicity measurements show well-known offsets between different scales (e.g., Kewley & Ellison 2008); however, in *each* scale, SNe Ic are more likely than SNe Ib to be found in metal-rich environments, while SNe Ic-bl (without observed GRBs) have environments that are similar in metallicity to those of both SNe Ib and SNe Ic. A Kolmogorov-Smirnov (K-S) test reveals that the probability that both the SN Ib and SN Ic local host-galaxy metallicities have been drawn from the same parent population is low: 1% (in PP04-O3N2), 7% (in KD02-comb),

---

[6] http://cfa-www.harvard.edu/iau/cbat.html .

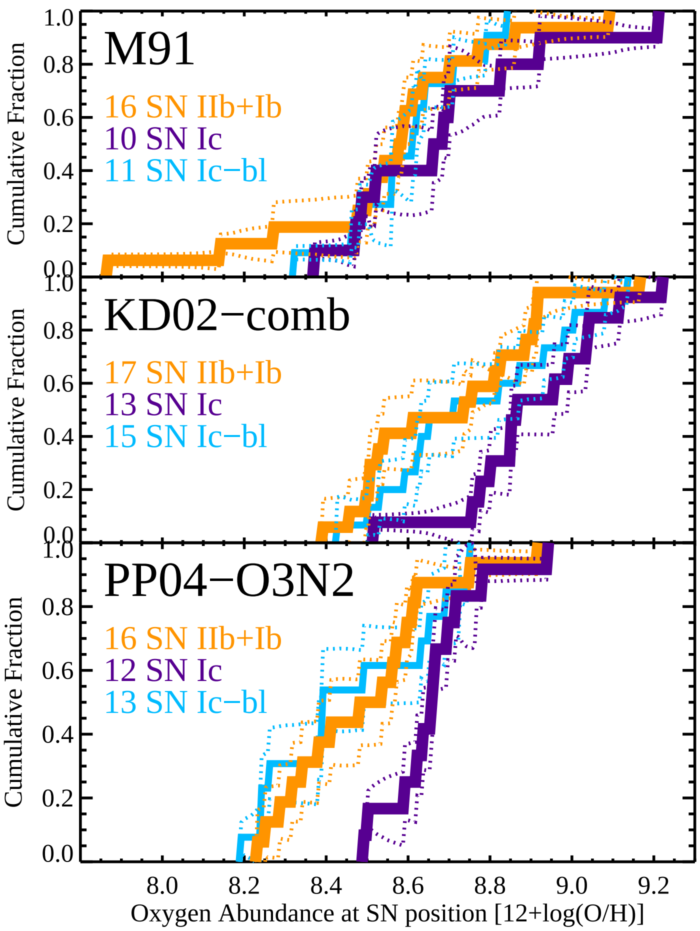

FIG. 1.— Cumulative fraction (solid lines) of measured oxygen abundances at the SN position of different types of CCSNe with three different metallicity diagnostics and their confidence bands (dotted lines, see text). SNe Ic (the demise of the most heavily stripped stars that lost much, if not all, of both their H and He layers) are systematically in more metal-rich environments than SNe Ib (SNe arising from less stripped stars that retained their He layer). This is a robust conclusion since the trend is independent of the adopted metallicity diagnostic. The PP04-O3N2 scale is least impacted by reddening and flux-calibration uncertainties. Note that in this study, the SN Ib subclass includes SNe IIb as well.

and 15% (in M91). The mean local metallicities in the PP04-O3N2 scale are 12 + log(O/H) = 8.49 ± 0.19 (for SNe Ib), with a standard deviation of the mean (SDOM) of 0.012; 8.66 ± 0.12 with SDOM of 0.010 (for SNe Ic); and 8.47 ± 0.21 with SDOM of 0.016 (for SNe Ic-bl). In all scales, SN Ic sites have oxygen abundances that are 0.14–0.20 dex higher than those of SN Ib.

Our results are somewhat at odds with those of Anderson et al. (2010), who find a slight and insignificant difference between environmental metallicities of SNe Ib and SNe Ic in their sample from only targeted SN searches. We have no SNe in common with their sample, and a detailed comparison of the two different samples is required to resolve the discrepancy, which is beyond the scope of this Letter.

5.1. *Tests for Possible Systematic Effects*

While there are selection effects that went into our heterogeneous sample, none of them is expected to affect SNe Ib systematically more than SNe Ic, and hence should not be able to cause our observed trend. We checked that the SN survey mode does not explain the observed trend; indeed, both SNe Ib and SNe Ic were drawn in almost equal proportions from both targeted and untargeted surveys (Table 1), and the relative difference in the metallicity of SN Ib and SN Ic environments is visible even when only comparing SNe from the same survey mode, albeit with more noise because of the smaller numbers of objects. Furthermore, we checked that both SNe Ib and SNe Ic span comparable redshift ranges, with median redshifts of 0.015 (for SNe Ib) and 0.017 (for SNe Ic). However, the broad-lined SNe Ic in our sample extend to larger redshifts, with a median of 0.043.

While some surveys may have difficulty discovering SNe in the central cores of bright galaxies, this detection difficulty does not appear to affect one SN type more than another in our SN sample: from Table 1, most of the SNe included here were found far from the central 1″, and those SNe that have offsets less than 1″ comprise all types (SN Ib, Ic, Ic-bl). The only strong selection effect in our sample is that we require H II region emission lines to be present at the SN position with which we can determine the ISM oxygen abundance, meaning that the SN location has to have had a large amount of recent (i.e., a few million years) star-formation activity. However, this requirement affects SNe Ib and SNe Ic equally since our objects sample the same redshift range.

5.2. *Supernova Progenitors with Metallicity-Driven Winds?*

A reasonable suggestion for why the environments of SNe Ic are more metal rich than those of SNe Ib is that metallicity-driven winds (Vink & de Koter 2005; Crowther & Hadfield 2006) in the progenitor stars prior to explosion are responsible for removing most, if not all, of the He layer whose spectroscopic nondetection distinguishes SNe Ic from SNe Ib. This explanation may favor the single massive WR progenitor scenario as the dominant mechanism for producing SNe Ib/c (Filippenko & Sargent 1985; Woosley et al. 1993), at least for those in large star-forming regions (§ 5.1). While the binary scenario has been suggested as the dominant channel for numerous reasons (see Smartt 2009 for a review; Smith et al. 2011), we cannot assess it in detail, since none of the theoretical studies (e.g., Eldridge et al. 2008, and references therein) predict the metallicity dependence of the subtype of stripped SN. However, our results are consistent with the suggestion of Smith et al. (2011) that SNe Ic may come from stars with higher metallicities (and masses) than SNe Ib, even if they are in binaries.

The distribution of the SNe Ic-bl is puzzling: SNe Ic-bl seem to occur at metallicities between those of SNe Ib and SNe Ic, except GRB-SNe which are found at very low metallicities (but see Soderberg et al. 2010; Levesque et al. 2010a; also see Levesque et al. 2010b for other GRB host metallicities). This may indicate another key ingredient beyond metallicity for producing ordinary SNe Ic-bl, perhaps magnetic fields.

We find only a factor of 5 difference between the lowest metallicity Z for SNe Ib and the highest metallicity for SNe Ic. Since the mass-loss rate $\dot{M}$ is proportional to $Z^{0.86}$ (Vink & de Koter 2005), this difference in Z would imply a *maximum* factor of 4 difference in $\dot{M}$ between SN Ib and SN Ic progenitors. The question remains whether this small difference in $\dot{M}$ is enough to be responsible for removing all of the He layer, or other factors are responsible that have a higher dependence on metallicity than line-driven winds, or the metallicity trend simply correlates with another property such as progenitor mass (Kelly et al. 2008; Anderson & James 2008) that may determine the SN outcome. All observations and theoretical work (see Bastian et al. 2010 for a review) indicate that the initial mass function is universal at the metallicities found herein.

Our results validate the independent hypothesis of Arcavi et al. (2010), which was based on indirect data: as an explanation for the fact that none of the 15 CCSNe found by the Palomar Transient Factory (PTF) in dwarf galaxies ($M_R < -18$ mag) was a SN Ic, Arcavi et al. (2010) suggest that SNe Ic do not occur at low metallicity since low-luminosity galaxies usually have low metallicity, in contrast to SNe Ic-bl of which two were found by PTF in dwarf hosts. Here we have supporting direct evidence; we show that SN Ic host environments have systematically higher metallicities than those of SNe Ib, while those of SNe Ic-bl encompass both low and high abundances. Nevertheless, it is important to measure metallicities directly and not rely on the host-galaxy luminosity (L) as a proxy, as we show next.

5.3. *The Need for Local Metallicity Measurements*

Since we possess direct local metallicity measurements, here we test whether SN host-galaxy luminosity and measured nuclear metallicity is a good proxy for the local SN metallicity, as assumed in some studies. To that end, we drew the SN host-galaxy luminosities from the Lyon-Meudon Extragalactic Database (HyperLEDA)[7] as their sample has been homogeneously compiled, and adopt their reported absolute B-band magnitudes, M_B, in Table 1. Note that the lowest-luminosity SN host galaxies are from untargeted surveys. Furthermore, 14 galaxies in our sample have nuclear SDSS spectra and their PP04 metallicities were taken from SDSS[8].

In Figure 2 we plot the measured oxygen abundance (on the PP04-O3N2 scale) at the position of stripped CCSN vs. the SN host-galaxy luminosity, and for comparison the oxygen abundance as would be inferred from the SDSS L–Z relationship (Tremonti et al. 2004) including 1σ uncertainties. For consistency, we have converted the L–Z relationship from Tremonti et al. (2004) to the scale of PP04-O3N2 using the empirical calibrations of Kewley & Ellison (2008). Figure 2 demonstrates that nuclear metallicity when derived from the SN host luminosity is not a good proxy for the local oxygen abundance of the environments of SNe: the local metallicities are often lower than the inferred central ones (because of metallicity gradients; van Zee et al. 1998), but also occasionally larger (e.g., Young et al. 2010), and in most cases more deviant than the 1σ metallicity uncertainties (i.e., 0.16 dex) would indicate from SDSS. The differences between the predicted central and the measured local metallicity values range from −0.4 dex to +0.5 dex (up to 3σ away from the SDSS L–Z value), with a median of 0.2 dex. Moreover, the nuclear PP04-O3N2 metallicities are deviant from the local values by an average of 0.13 dex, with extremes as large as 0.24 dex, and always more deviant than our measured uncertainties. Thus, we conclude that nuclear metallicities are not a good measure of local metallicities.

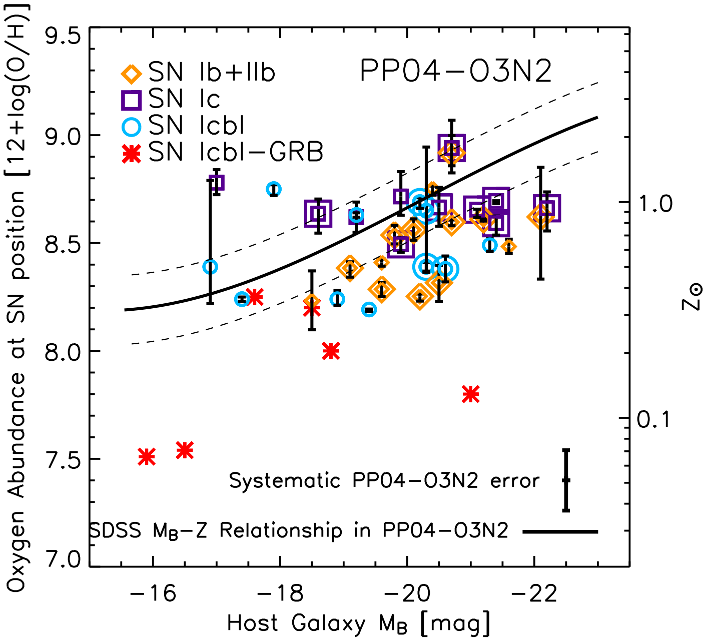

Fig. 2.— Measured oxygen abundance at the position of different SN types vs. the SN host-galaxy luminosity, and for comparison the oxygen abundance as inferred from the SDSS L–Z relationship (Tremonti et al. 2004), converted to PP04-O3N2 (solid line) including 1σ uncertainties (dashed lines). The nuclear metallicity as derived from the SN host luminosity using the SDSS relationship is not a good proxy for the local oxygen abundance of SN environs. Here, we adopt a solar oxygen abundance of 12 + log(O/H) = 8.69 (Asplund et al. 2009), but note that the exact value of the solar abundance has no impact on our conclusions. SNe found in targeted SN surveys are designated by extra circles, squares, and diamonds. The representative systematic error of 0.14 dex for the PP04-O3N2 scale is shown in the bottom-right corner.

6. CONCLUSIONS

We present a statistically significant sample of 35 new host-galaxy spectra of stripped CCSN (SNe IIb and Ib, SNe Ic, and SNe Ic-bl), and in combination with published host-galaxy spectra, we perform robust, uniform, and direct determination of their local metallicity. The aim is to search for metallicity trends that may let us differentiate between various debated SN Ib/c progenitor scenarios. We find that the environments of SNe Ic are systematically more metal rich in three scales than those of SNe Ib (on average by 0.14–0.20 dex in all scales), with a K-S test yielding very small probabilities that they are drawn from the same parent population. We also show that SNe Ic-bl (without GRBs) are intermediate to those other classes.

---

[7] http://leda.univ-lyon1.fr/ .

[8] http://www.mpa-garching.mpg.de/SDSS/DR7

For the future, we recommend this kind of detailed local metallicity study for all subtypes of CCSNe from galaxy-impartial, large, and deep photometric surveys (e.g., PTF, Pan-STARRS, Skymapper, LSST) in order to comprehensively understand the impact of metallicity on massive stellar death, as well as to compute cosmologically important parameters, such as SN rates, as a function of metallicity.

Note added in proof: After our manuscript was accepted, Leloudas et al. (2011) appeared on the arXiv-server on a similar topic. While we corrected one SN identification based on their work, we are not able to make more comparisons at this time.

We thank the referee, J. Brinchmann, for helpful comments that improved the manuscript, and R. C. Thomas and J. Marriner for refining via SNID (Blondin & Tonry 2007) the subtypes of some of the CCSNe included in this study. We thank R. J. Foley, R. Chornock, T. N. Steele, and D. Poznanski for helping to obtain some spectra, and D. Rupke and N. Smith for useful discussions. M.M. acknowledges support from the Miller Institute at UC Berkeley and from Hubble Fellowship grant HST-HF-51277.01-A, awarded by STScI, which is operated by AURA under NASA contract NAS5-26555. L.K. acknowledges support from NSF Early CAREER award AST–0748559. A.V.F.'s group is grateful for financial assistance from the TABASGO Foundation and NSF grant AST–0908886. J.S.B. and D.A.P. were partially supported by a DOE SciDAC grant and HST-GO-11551. The data presented herein were obtained at the W. M. Keck Observatory, which is operated as a scientific partnership among the California Institute of Technology, the University of California, and NASA; the observatory was made possible by the generous financial support of the W. M. Keck Foundation.

REFERENCES

Anderson, J. P., Covarrubias, R. A., James, P. A., Hamuy, M., & Habergham, S. M. 2010, MNRAS, 407, 2660
Anderson, J. P., & James, P. A. 2008, MNRAS, 390, 1527
Arcavi, I., et al. 2010, ApJ, 721, 777
Asplund, M., Grevesse, N., Sauval, A. J., & Scott, P. 2009, ARA&A, 47, 481
Bastian, N., Covey, K. R., & Meyer, M. R. 2010, ARA&A, 48, 339
Blondin, S., & Tonry, J. L. 2007, ApJ, 666,1024
Boissier, S., & Prantzos, N. 2009, A&A, 503, 137
Cardelli, J. A., Clayton, G. C., & Mathis, J. S. 1989, ApJ, 345, 245
Chornock, R., et al. 2010, ApJ, submitted, (arXiv:1004.2262)
Christensen, L., Vreeswijk, P. M., Sollerman, J., Thöne, C. C., Le Floc'h, E., & Wiersema, K. 2008, A&A, 490, 45
Clocchiatti, A., Wheeler, J. C., Brotherton, M. S., Cochran, A. L., Wills, D., Barker, E. S., & Turatto, M. 1996, ApJ, 462, 462
Crowther, P. A., & Hadfield, L. J. 2006, A&A, 449, 711
Eldridge, J. J., Izzard, R. G., & Tout, C. A. 2008, MNRAS, 384, 1109
Filippenko, A. V. 1997, ARA&A, 35, 309
Filippenko, A. V., Li, W. D., Treffers, R. R., & Modjaz, M. 2001, in Small-Telescope Astronomy on Global Scales, ed. W. P. Chen, C. Lemme, & B. Paczyński (San Francisco: ASP), 121
Filippenko, A. V., & Sargent, W. L. W. 1985, Nature, 316, 407
Gal-Yam, A., et al. 2005, ApJ, 630, L29
Kelly, P. L., Kirshner, R. P., & Pahre, M. 2008, ApJ, 687, 1201
Kewley, L. J., & Dopita, M. A. 2002, ApJS, 142, 35
Kewley, L. J., & Ellison, S. L. 2008, ApJ, 681, 1183
Leloudas, G., et al. 2011, A & A, submitted (arXiv:1102.2249)
Levesque, E. M., Kewley, L. J., Berger, E., & Jabran Zahid, H. 2010b, AJ, 140, 1557
Levesque, E. M., et al. 2010, ApJ, 709, L26
Matheson, T., et al. 2008, AJ, 135, 1598
Maund, J. R., Smartt, S. J., & Schweizer, F. 2005, ApJ, 630, L33
McGaugh, S. S. 1991, ApJ, 380, 140
Modjaz, M., et al. 2008, AJ, 135, 1136
Modjaz, M., et al. 2009, ApJ, 702, 226
Nomoto, K., Tominaga, N., Umeda, H., Maeda, K., Ohkubo, T., & Deng, J. 2006, Nuclear Physics A, 777, 424
Oke, J. B., et al. 1995, PASP, 107, 375
Pastorello, A., et al. 2007, Nature, 447, 829
Pérez-Montero, E. & Díaz, A. I. 2003, MNRAS, 346, 105
Pettini, M., & Pagel, B. E. J. 2004, MNRAS, 348, L59
Podsiadlowski, P., Langer, N., Poelarends, A. J. T., Rappaport, S., Heger, A., & Pfahl, E. 2004, ApJ, 612, 1044
Prantzos, N., & Boissier, S. 2003, A&A, 406, 259
Prieto, J. L., Stanek, K. Z., & Beacom, J. F. 2008, ApJ, 673, 999
Rupke, D., Kewley, L. J., & Chien, L.-H., 2010, ApJ, 723, 1255
Sahu, D. K., Tanaka, M., Anupama, G. C., Gurugubelli, U. K., & Nomoto, K. 2009, ApJ, 697, 676
Silverman, J. M., Mazzali, P., Chornock, R., Filippenko, A. V., Clocchiatti, A., Phillips, M. M., Ganeshalingam, M., & Foley, R. J. 2009, PASP, 121, 689
Smartt, S. J. 2009, ARA&A, 47, 63
Smith, N., Li, W., Filippenko, A. V., & Chornock, R. 2011, MNRAS, in press (arXiv:1006.3899)
Soderberg, A. M., et al. 2010, Nature, 463, 513
Starling, R. L. C., et al. 2011, MNRAS, in press (arXiv:1004.2919)
Stritzinger, M., et al. 2009, ApJ, 696, 713
Thöne, C. C., Michałowski, M. J., Leloudas, G., Cox, N. L. J., Fynbo, J. P. U., Sollerman, J., Hjorth, J., & Vreeswijk, P. M. 2009, ApJ, 698, 1307
Tremonti, C. A., et al. 2004, ApJ, 613, 898
van Zee, L., Salzer, J. J., Haynes, M. P., O'Donoghue, A. A., & Balonek, T. J. 1998, AJ, 116, 2805
Vink, J. S., & de Koter, A. 2005, A&A, 442, 587
Woosley, S. E., & Bloom, J. S. 2006, ARA&A, 44, 507
Woosley, S. E., Langer, N., & Weaver, T. A. 1993, ApJ, 411, 823
Young, D. R., et al. 2010, A&A, 512, A70

TABLE 1
The Sample of Stripped-Envelope CCSNe

SN Name	SN Type	SN Host Galaxy	Redshift z	Galaxy M_B [mag]	M91$_{\mathrm{SNpos}}$ log(O/H)+12	KD02-comb$_{\mathrm{SNpos}}$ log(O/H)+12	PP04-O3N2$_{\mathrm{SNpos}}$ log(O/H)+12	SN Disc-typ
1990U	Ic	NGC7479	0.00794	-21.7	···	$9.04^{+0.24}_{-0.09}$	···	T
1991ar	Ib	IC49	0.01521	-20.1	$8.52^{+0.24}_{-0.11}$	$8.76^{+0.17}_{-0.02}$	$8.56^{+0.05}_{-0.05}$	T
1996D	Ic	NGC1614	0.01582	-21.4	$8.66^{+0.26}_{-0.06}$	$8.87^{+0.29}_{-0.19}$	$8.59^{+0.03}_{-0.06}$	T
1996aq	Ib	NGC5584	0.00547	-19.8	$8.59^{+0.10}_{-0.12}$	$8.92^{+0.04}_{-0.04}$	$8.54^{+0.04}_{-0.04}$	T
1997B	Ic	IC438	0.01041	-20.7	···	$9.22^{+0.04}_{-0.04}$	$8.94^{+0.13}_{-0.12}$	T
1999cn	Ic	MCG+02-38-043	0.02231	-19.9	$8.69^{+0.14}_{-0.07}$	$8.76^{+0.14}_{-0.02}$	$8.49^{+0.03}_{-0.04}$	T
1999di	Ib	NGC776	0.01641	-21.2	$9.09^{+0.03}_{-0.03}$	$9.17^{+0.06}_{-0.05}$	$8.94^{+0.07}_{-0.06}$	T
1999dn	Ib	NGC7714	0.00933	-20.5	$8.54^{+0.17}_{-0.20}$	$8.39^{+0.13}_{-0.05}$	$8.32^{+0.08}_{-0.09}$	T
2001ig	IIb	NGC7424	0.00292	-19.6	$8.27^{+0.07}_{-0.27}$	$8.53^{+0.09}_{-0.11}$	$8.29^{+0.03}_{-0.03}$	T
2002bl	Ic-bl	UGC5499	0.01591	-20.3	$8.79^{+0.40}_{-0.39}$	$9.01^{+0.31}_{-0.51}$	$8.65^{+0.29}_{-0.29}$	T
2004fe	Ic	NGC132	0.01788	-21.1	$9.21^{+0.79}_{-0.91}$	$8.14^{+0.87}_{-0.83}$	$8.65^{+0.00}_{-0.04}$	T
2004gt	Ic	NGC4038	0.00555	-21.4	$8.92^{+0.06}_{-0.05}$	$8.99^{+0.14}_{-0.12}$	$8.70^{+0.00}_{-0.01}$	T
2005eo	Ic	UGC04132	0.01743	-22.2	$8.49^{+0.51}_{-0.03}$	$8.78^{+0.44}_{-0.24}$	$8.66^{+0.08}_{-0.10}$	T
2005mf	Ic	UGC04798	0.01891	-20.5	$8.83^{+0.15}_{-0.36}$	$8.96^{+0.07}_{-0.20}$	$8.66^{+0.09}_{-0.09}$	T
2006jc	Ib-n	UGC04904	0.00548	-15.9	···	$8.78^{+0.03}_{-0.03}$	$8.42^{+0.04}_{-0.05}$	T
2007cl	Ic	NGC6479	0.02218	-20.9	···	$9.12^{+0.22}_{-0.05}$	···	T
2007gr	Ic	NGC1058	0.00173	-18.6	$8.37^{+0.58}_{-0.10}$	$8.52^{+0.53}_{-0.32}$	$8.64^{+0.07}_{-0.09}$	T
2007rw	IIb	UGC7798	0.00857	-19.1	$8.58^{+0.15}_{-0.03}$	$8.54^{+0.26}_{-0.12}$	$8.38^{+0.03}_{-0.04}$	T
2007uy	Ib	NGC2770	0.00700	-20.7	$8.70^{+0.10}_{-0.04}$	$8.83^{+0.11}_{-0.09}$	$8.60^{+0.01}_{-0.02}$	T
2008D	Ib	NGC2770	0.00700	-20.7	$8.86^{+0.06}_{-0.00}$	$8.81^{+0.07}_{-0.02}$	$8.92^{+0.08}_{-0.06}$	T
2008cx	IIb	NGC309	0.01890	-22.1	$7.87^{+1.19}_{-0.96}$	$8.50^{+0.75}_{-0.29}$	$8.62^{+0.23}_{-0.29}$	T
2005az	Ic	NGC4961	0.00875	-19.2	$8.52^{+0.20}_{-0.20}$	$8.80^{+0.08}_{-0.08}$	$8.62^{+0.07}_{-0.07}$	Non-T
2005kf	Ic	SDSSJ074726.40+265532.4	0.01508	-17.0	$8.70^{+0.08}_{-0.18}$	$9.04^{+0.02}_{-0.07}$	$8.78^{+0.06}_{-0.06}$	Non-T
2006fo	Ib	UGC02019	0.02074	-20.4	$8.77^{+0.17}_{-0.13}$	$8.88^{+0.21}_{-0.19}$	$8.75^{+0.01}_{-0.03}$	Non-T
2006ip	Ic	2MASXJ23483173-0208524	0.03062	-19.9	$8.47^{+0.24}_{-0.29}$	$8.85^{+0.07}_{-0.06}$	$8.72^{+0.12}_{-0.09}$	Non-T
2006jo	Ib	SDSSJ012314.96-001948.8	0.07678	-21.6	$8.61^{+0.09}_{-0.09}$	$8.91^{+0.03}_{-0.03}$	$8.48^{+0.03}_{-0.03}$	Non-T
2006ld	Ib	UGC348	0.01394	-18.5	$8.63^{+0.26}_{-0.03}$	$8.61^{+0.18}_{-0.30}$	$8.23^{+0.14}_{-0.14}$	Non-T
2006lt	Ib	NSFJ021659.89+304157.4	0.01602	···	$8.59^{+0.13}_{-0.11}$	$8.73^{+0.08}_{-0.07}$	$8.57^{+0.06}_{-0.05}$	Non-T
2007eb	Ic-bl	NSFJ224248.98+240247.2	0.04262	···	$8.32^{+0.28}_{-0.33}$	$8.43^{+0.31}_{-0.08}$	$8.26^{+0.07}_{-0.07}$	Non-T
2007eq	Ib	NSFJ234805.93+281420.2	0.02964	···	$8.50^{+0.23}_{-0.18}$	$8.51^{+0.14}_{-0.18}$	$8.34^{+0.09}_{-0.08}$	Non-T
2007fj	Ic	APMUKS B221135.36-2826	0.05680	···	···	$8.85^{+0.05}_{-0.05}$	$8.50^{+0.04}_{-0.04}$	Non-T
2007gx	Ic-bl	NSFJ171851.49+224716.6	0.07894	···	···	$9.14^{+0.02}_{-0.02}$	···	Non-T
2007jy	Ib	SDSSJ205121.43+002357.8	0.18295	-19.6	$8.48^{+0.05}_{-0.05}$	$8.92^{+0.01}_{-0.01}$	$8.41^{+0.02}_{-0.02}$	Non-T
2007qw	Ic-bl	SDSSJ223529.00+002856.1	0.15064	-19.4	$8.46^{+0.06}_{-0.04}$	$8.50^{+0.10}_{-0.06}$	$8.19^{+0.00}_{-0.01}$	Non-T
2008cw	IIb	SDSSJ163238.15+412730.7	0.03193	-18.3	···	$8.46^{+0.01}_{-0.01}$	···	Non-T
1997ef[b]	Ic-bl	UGC4107	0.01169	-20.2	$8.84^{+0.02}_{-0.03}$	$8.93^{+0.04}_{-0.04}$	$8.69^{+0.02}_{-0.03}$	T
1998ey[b]	Ic-bl	NGC7080	0.01610	-21.8	···	$9.08^{+0.04}_{-0.04}$	···	T
2002ap[b]	Ic-bl	NGC628	0.00220	-20.6	$8.56^{+0.07}_{-0.07}$	$8.62^{+0.06}_{-0.06}$	$8.38^{+0.06}_{-0.06}$	T
2003jd[b]	Ic-bl	MCG-01-59-21-20.3	0.01880	-20.3	$8.62^{+0.02}_{-0.02}$	$8.59^{+0.05}_{-0.05}$	$8.39^{+0.02}_{-0.02}$	T
2007ru[c]	Ic-bl	UGC12381	0.02218	-20.3	···	$8.98^{+0.04}_{-0.04}$	···	T
2007Y[d]	Ib	NGC1187	0.00464	-20.2	$8.14^{+0.13}_{-0.07}$	$8.51^{+0.23}_{-0.15}$	$8.25^{+0.01}_{-0.02}$	T
2005kr[b]	Ic-bl	SDSSJ030829.66+005320.1	0.13450	-17.4	$8.64^{+0.01}_{-0.01}$	$8.63^{+0.03}_{-0.03}$	$8.24^{+0.01}_{-0.01}$	Non-T
2005ks[b]	Ic-bl	SDSSJ213756.52-000157.7	0.09870	-19.2	$8.71^{+0.03}_{-0.04}$	$8.87^{+0.02}_{-0.03}$	$8.63^{+0.01}_{-0.01}$	Non-T
2005nb[b]	Ic-bl	UGC7230	0.02377	-21.3	$8.56^{+0.03}_{-0.03}$	$8.65^{+0.08}_{-0.09}$	$8.49^{+0.03}_{-0.03}$	Non-T
2006nx[b]	Ic-bl	SDSSJ033330.43-004038.0	0.13700	-18.9	$8.48^{+0.09}_{-0.10}$	$8.53^{+0.10}_{-0.14}$	$8.24^{+0.04}_{-0.03}$	Non-T
2006qk[b]	Ic-bl	SDSSJ222532.38+000914.9	0.05840	-17.9	$8.61^{+0.07}_{-0.08}$	$8.82^{+0.04}_{-0.05}$	$8.75^{+0.02}_{-0.03}$	Non-T
2007I[b]	Ic-bl	SDSSJ115913.13-013616.1	0.02160	-16.9	···	$8.71^{+0.03}_{-0.04}$	$8.39^{+0.40}_{-0.17}$	Non-T

Note. — SNe above the horizontal line: Local host-galaxy spectra are presented and analyzed here for the first time. SNe below the horizontal line: we measu
line fluxes and computed oxygen abundances from previously published spectra.

[a] SN Discovery Type: T = SN host galaxy was targeted; Non-T = SN host galaxy was not targeted.

[b] Sample and data from Modjaz et al. (2008), which uses the same technique as this work.

[c] Remeasured from spectrum in Sahu et al. (2009).

[d] Measured from spectrum in Stritzinger et al. (2009).